Letters in High Energy Physics Volume 2024
ISSN: 2632-2714

Synthesis and Photoluminescence of the Self-Activated Garnet Phosphor Triggered by Eu^{3+} for Blue-Red Luminescence

Ganesh C. Vandile[a]*, Deoram V. Nandanwar[a]*, Amar K. Nandanwar[b]*, Bhupendra R. Walde[a]

[a]Shri Mathuradas Mohota College of Science, Nagpur-440009, India.

[b]J. M. Patel Arts, Commerce & Science College, Bhandara-441904, India.

Corresponding Author: (D. V. Nandanwar) dvnandanwar@gmail.com

(G. C. Vandile) ganesh9326wandile@gmail.com

(A. K. Nandanwar) amarknjmpc@gmail.com

Abstract:

The red-emitting phosphors were attracting very much interest in the fields of lighting devices. Therefore, we have prepared $LiCa_3ZnV_3O_{12}:Eu^{3+}$ by using a simple high temperature solid-state reaction. The garnet has cubic structure that was confirmed by XRD and Rietveld refinements. The photoluminescence properties were demonstrated by emission and excitation of the samples. The excitation wavelength was 344 nm for both VO_4^{3-} and Eu^{3+} in the UV region while emission peaks were found at 490 nm due to VO_4^{3-} and at 592 nm, 611 nm and 633 nm due to Eu^{3+} but dominant peak was obtained at 611 nm in the transition from $^5D_0$ to $^7F_1$. The blue emission was confirmed by CIE chromaticity with coordinated (0.239, 0.329) and CCT was 17210 K for vanadate garnet. The surface analysis was analyzed by FE-SEM and compositional analysis was analyzed by EDX. The energy bandgap of the sample was studied by UV-VIS spectroscopy and it was found as 3.72 eV for absorbance wavelength 334 nm of the host sample. The investigation for bond length and nature of bonds in the samples were carried out with FTIR spectroscopy. For thermal stability and transitional temperature were studied by TGA/DTA analysis. The garnet phosphors that have been prepared can be applicable in the production of red and blue lighting devices, white lighting devices, optical temperature sensors, active powder in solid-state lasers, and CRTs.

Keywords: Self-activated, garnet phosphor, UV-VIS absorbance, Eu^{3+}- doped garnet, vanadate garnet.

Introduction

According to economic demand, energy is essential for modern life. The researchers have been always looking for more efficient energy sources. They are focusing on improving solid-state light sources with new garnets due to their superior properties and color rendering. Last twenty year ago, they have thought that inorganic compounds with a garnet structured phosphor would be great for optical uses because they have rigid lattices and can transfer heat well [1]. The formula for garnet is $A_3B_2C_3O_{12}$ where, A, B, and C cations have different shapes, sizes, and valences, which lead to a wide range of compositions. Due to change in shape, size & valances, it can lead to changes in crystal field strength, symmetry, and electronic structures [2]. These can have a hug impact on how energy is splitted and how electrons move in a garnet phosphor that contains a rare earth activator [3]. Where, A is without inversion symmetry while B & C are with inversion symmetry [4]. Also, A, B, and C has occupied for dodecahedral, octahedral, and tetrahedral sites, respectively. Generally, the garnet phosphor are possessing cubic structure and having Ia-3d as space group with international space group number 370. The garnet contained vanadate which has unique property to emit bluish light when it is irradiated by UV radiation [5]. Therefore, it is preferred to include in the host to energy transfer (ET) due to single dopant.

The composition of garnet with vanadate allows efficient energy transfer from their energy absorption to trivalent lanthanide activators. Vanadate VO_4^{3-} based garnet compounds like $A3B2(VO_4)_3$ have been

studied. Due to their intrinsic luminescence, these garnets have become a growing research field [6]. Vanadate garnet has cubic in crystal structure compounds which received more attention. The CT transition from V^{5+} to O^{2-} in the tetrahedral [VO_4] structure causes intense visible emission from these phosphors, which absorb UV and near-UV light [7]. The vanadate phosphor's [VO_4] had a good luminescent center [8]. The doping of Ln^{3+} ions into vanadate hosts result that ET from [VO_4^{3-}] groups to Ln^{3+} ions which become brighter luminescence. Recently, garnet structured vanadate phosphors like $LiCa_3MgV_3O_{12}$, $LiCa_3MgV_3O_{12}:Eu^{3+}$ and LiCa3ZnV3O12:Nd^{3+} have been studied for optical applications. $Ca_3LiMgV_3O_{12}:Eu^{3+}$ [9], $LiCa_3MgV_3O_{12}:Sm^{3+}$ [10], $LiCa_3MgV_3O_{12}:Bi^{3+}$ [11], $LiCa_3MgV_3O_{12}:Er^{3+}$ [12], $LiCa_3MgV_3O_{12}$: Nd^{3+}/Yb^{3+} [13], Bi^{3+}/Eu^{3+} garnet phosphors for full-color luminescence tuning [14]. However, Eu^{3+} photoluminescence in $LiCa_3ZnV_3O_{12}$ matrix is not reported.

In recent years, there have been useful investigations done on rare earth-doped garnets phosphor that include phosphors with emitting yellow, green, blue, and red light [15]. These phosphors have the potential to be used in white light emitting diodes (w-LEDs). Within this group of rare earth, there is a persistent interest in the synthesis of garnets that have been triggered by Eu^{3+} for the purpose of producing red-emitting phosphors [16]. The europium was applicable in phosphor materials for luminescence due to their numerous advantages, including high color purity as well as luminescence efficiency [17]. Eu^{3+} ions have been extensively used in solid-state lighting [18]. Furthermore, a pure white light can be easily achieved by using these rare earth metal Eu^{3+} as luminescent ions (activator). Fluorescent lamps and white lighting devices have been developed by using solely these elements as luminescent centers within oxide, nitride, or sulfide lattices [19]. Nevertheless, Eu^{3+} ions with vanadate exhibit narrow excitation spectra owing to the forbidden 4f–4f transitions, leading to optimum absorbance [20].

As results, the present research article investigates the applications of phosphor by concentrating on the photoluminescence and thermal properties of Eu^{3+}-doped self-activated ($LiCa_3ZnV_3O_{12}$) vanadate garnet phosphor. This phosphor was prepared using the high temperature solid state reaction, and the vanadate garnet group VO_4^{3-} was used as the sensitizer in host. This method transferred the absorbed energy from VO_4^{3-} to the activators Eu^{3+}, which resulted in a wide range of blue emission due to VO_4^{3-} and red emission due to Eu^{3+}. The analysis of emission spectra ranging from near ultraviolet to visible light has provided a comprehensive understanding of the complex mechanisms that underlie ET.

2. Experiments

2.1. Material Preparation

By using the SSR technique, a series of $LiCa_3ZnV_3O_{12}:xEu^{3+}$ were synthesized, with x = 0, 0.2 to 0.5, 1, 2, 3, and 5%. The stoichiometric ratio was used to determine the weight of the raw materials Li_2CO_3, $CaCO_3$, ZnO, and NH_4VO_3. When the mixture had been ground for approximately thirty-forty minutes using an agate mortar and pestle, it was then transferred to a muffle furnace and sintered twice. The two conditions for sintering were 650 degrees Celsius for two hours and 950 degrees Celsius for six hours, respectively. The prepared samples were ground into powders so that they could be used in subsequent investigations.

2.2. Characterization Techniques

The X-ray powder diffraction patterns of samples were investigated by X-ray diffractometer (Rigaku Miniflex 600, 40kV and 30mA, Cu Kα wavelength 0.154059 nm) was used to identify the phase. FE-SEM (JEOL, JSM-6500F) with an 80W Xe light source and a 25 kV high tension voltage between the anode and cathode as electron accelerating voltage that is used to optimize the topographical and compositional characterizations. FTIR spectroscopy was recorded for identification and nature bonds by BRUKER (Alpha II). TGA/DTA was done by SHIMADZU (DTC-60) to investigate about thermal stability of sample. The energy bandgap was determined from UV-VIS absorbance spectra which are demonstrated by UV-VIS Spectrophotometer (Lasany LI-285). Using a photomultiplier tube operating at a 135W Xenon lamp as the excitation lamp, the excitation and emission spectra were

recorded at room temperature using FS5 fluorescence spectrometer. Color chromaticity data were used to calculate and color coordinates and CCT.

3. Results and Discuss

3.1. XRD

Figure 1 shows the XRD patterns of the host $LiCa_3ZnV_3O_{12}$ as well as $LiCa_3ZnV_3O_{12}:Eu^{3+}$ compounds that have Eu^{3+} added to them. There are no impurities in the specimens, so the peaks are all the same as on the standard card. It was seen that the diffraction patterns of the synthesized sample were similar, which means that all of the peaks fit with the pure crystalline phase of the $LiCa_3ZnV_3O_{12}$ vanadate matrix. There is no appreciable in the pattern of XRD due to doping into the samples. The unit cell structure of LCZVO host is the cubic structure in the Ia-3d space group. CaO_8 dodecahedral are formed by connecting Ca atoms with eight O atoms. ZnO_6 octahedral are formed by Zn atoms and six O atoms. V atoms are found in the center of VO_4 tetrahedral. Figure 2 shows the XRD with Rietveld refinement results of a typical LCZVO phosphor. The results of the refinement are reliable because the factors are low (R_p = 9.136, R_w = 7.364, R_{we} = 4.361, and χ^2 = 2.361). The results show that the samples were made pure, and adding Eu^{3+} ions in the right way doesn't change the purity of the phase.

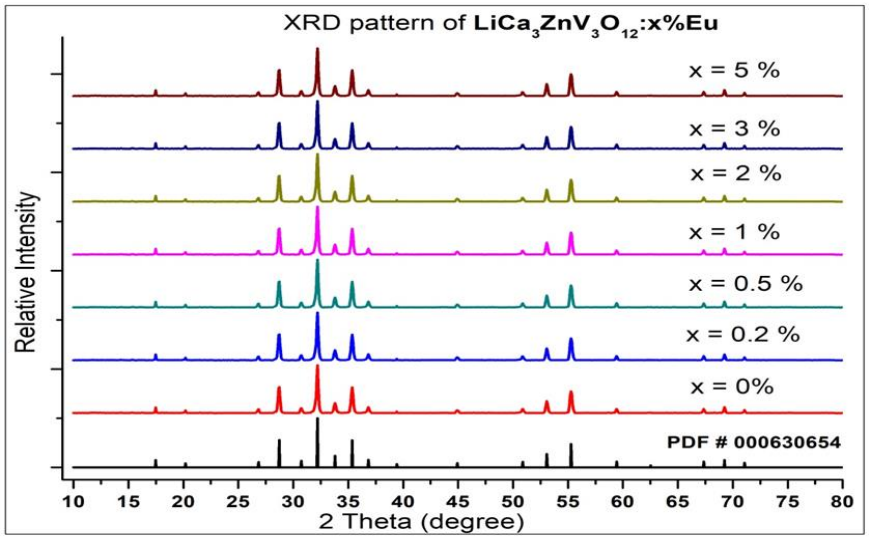

Figure 1: XRD pattern for $LiCa_3ZnV_3O_{12}$ host as well as $LiCa_3ZnV_3O_{12}:Eu^{3+}$.

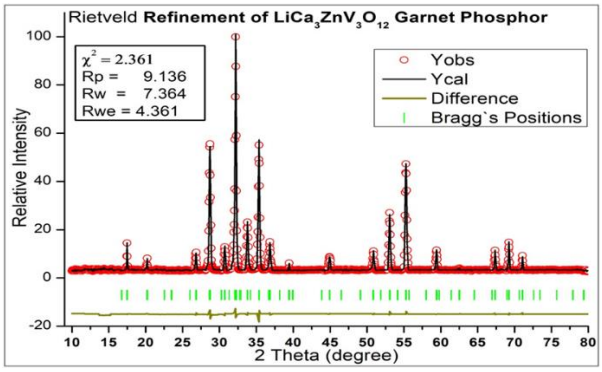

Figure 2: XRD pattern with Rietveld refinement of $LiCa_3ZnV_3O_{12}$ garnet phosphor.

3.2. Morphology and EDX

Figure 3 displays SEM images of $LiCa_3ZnV_3O_{12}:Eu^{3+}$ obtained from a FESEM at varying magnifications. Investigating the grain size and surface study can be accomplished with the help of this technique. The EDX technique is used to characterize the sample in order to investigate the elemental composition of the material. Figure 4 demonstrates that all of the elements are present and the composition is as desired. The host materials Ca, Zn, V, and O, in addition to the dopant Eu^{3+} ions, are shown to have energy dispersive peaks. Lithium has a relatively low atomic mass therefore; it is not shown in the representation.

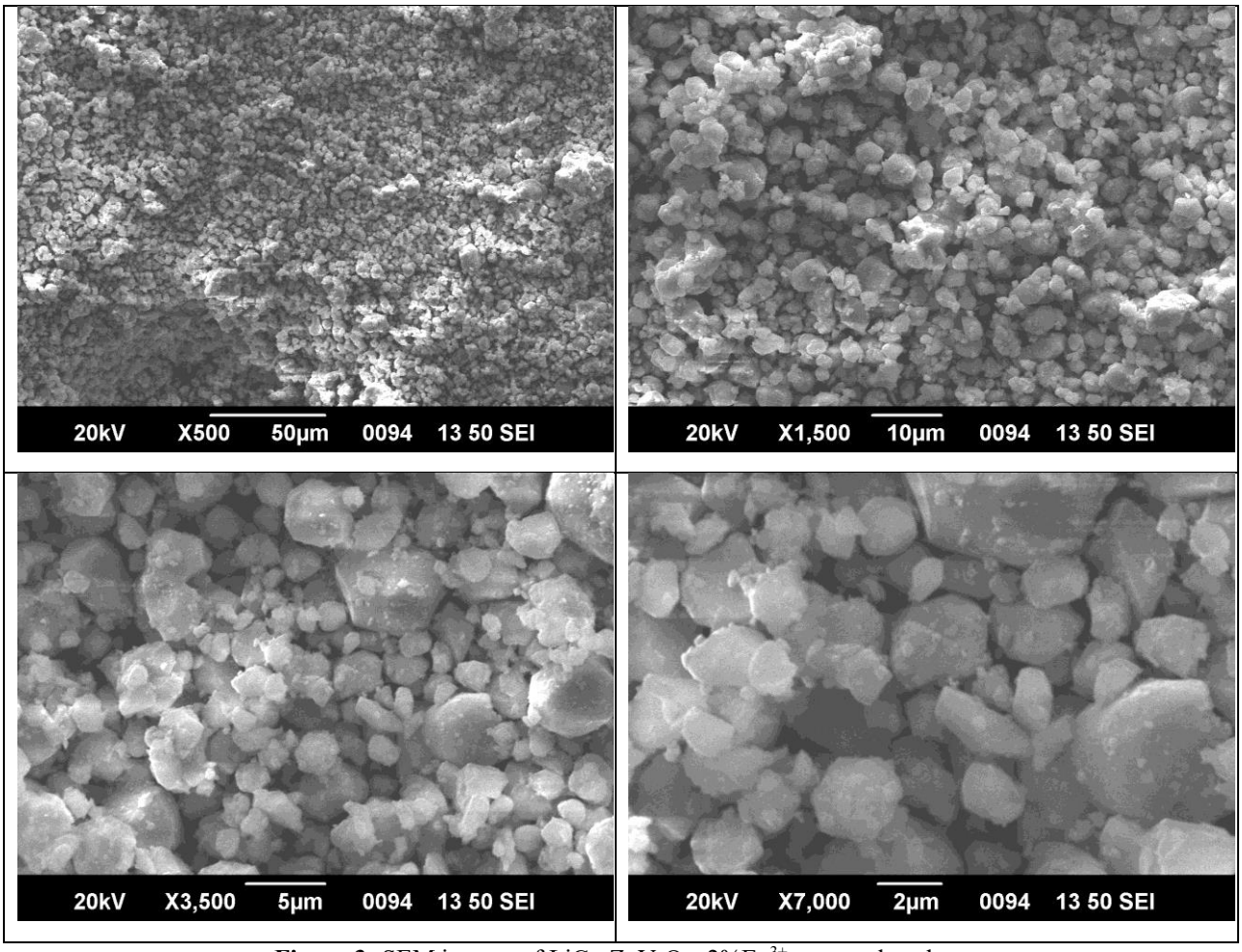

Figure 3: SEM images of $LiCa_3ZnV_3O_{12}$:2%Eu^{3+} garnet phosphor.

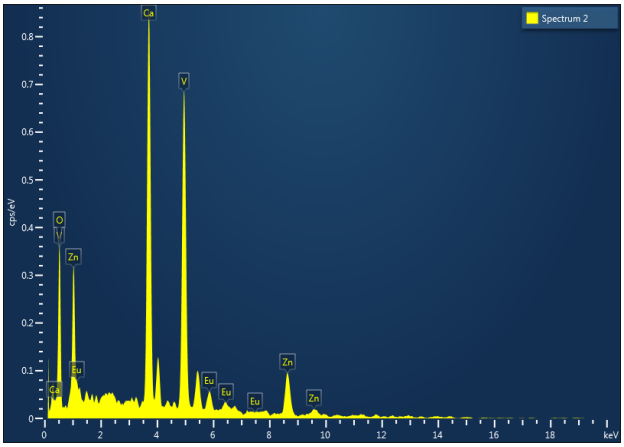

Figure 4: Energy Dispersive X-ray Spectrum of $LiCa_3ZnV_3O_{12}$:2%Eu^{3+} garnet phosphor.

3.3. TGA/DTA

The TGA/DTA analysis has been demonstrated to investigate the thermal stability, transition temperature, and melting point of the $LiCa_3ZnV3O_{12}$. The TGA/DTA analysis was performed for the sample at temperatures ranging from room temperature to 900 degrees Celsius. After reaching a temperature of 150 degrees Celsius, the DTA curve of the sample displayed a plateau region that was parallel to the temperature axis till reaching 471 degree Celsius, after that it goes decreasing, is shown in Figure 5. There are two plateau regions for TGA curves at 203 degrees Celsius and 807 degrees Celsius is shown in Figure 5.

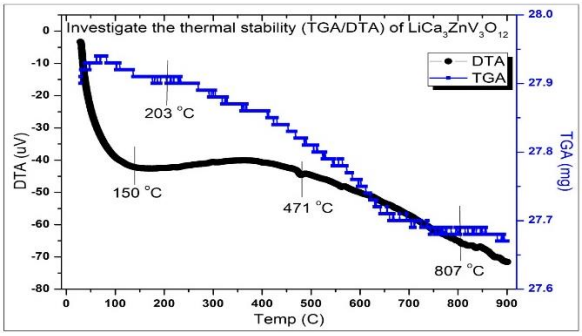

Figure 5: TGA/DTA curve of the $LiCa_3ZnV_3O_{12}$ garnet phosphor.

3.4. Fourier Transforms Infrared Spectroscopy (FTIR)

As seen in Figure 6, FTIR spectroscopy was performed at 950 °C using a Fourier transform spectrometer. The FTIR revealed absorption peaks at lower regions, approximately 500 cm^{-1} to 1000 cm^{-1}, which correspond to pure metal-oxide bonds, such as the Ca–O (metal–oxygen), Cd–O, and Li–O metal bonds formed for $LiCa_3ZnV_3O_{12}$. Presence of moisture in the sample was responsible for the development of the peaks at 2855cm^{-1} and 2922 cm^{-1}. Nitrate peaks have been noticed in the absorption peaks at 1758 cm^{-1}, 2023 cm^{-1} and 2378 cm^{-1}. The existence of bending frequency Ca–O and Zn–O vibrational motions contributed for the absorptions at approximately 756 cm^{-1} and 855 cm^{-1} [21]. The bending and vibrations of the V–O and Li–O bonds in $LiCa_3ZnV_3O_{12}$ were the cause of the absorption peaks at 540 cm^{-1} and 785 cm^{-1} respectively [22].

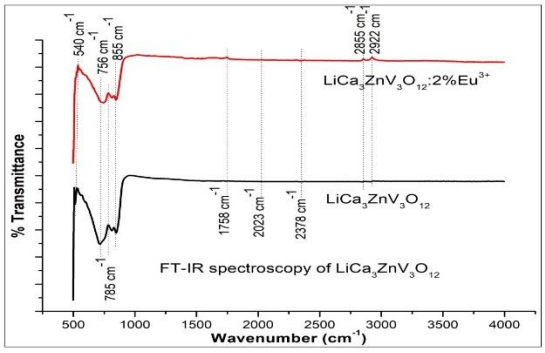

Figure 6: FT-IR spectroscopy of $LiCa_3ZnV_3O_{12}$ sintered at different 950 ºC recorded in the range of 500 cm−1 to 4000 cm^{-1}

3.5. UV-VIS Spectroscopy

One molar mass of $Ca_3LiZnV3O_{12}$:xEu^{3+} was used to prepare the solution with DMSO as base.

Figure 7 shows the UV–VIS absorbance spectrum that was recorded to investigate the energy bandgap of host sample. It is also carried out for absorbance of $Ca_3LiZnV3O_{12}$:xEu^{3+}. The results showed that absorption peaks ranging from approximately 250–375 nm. It was the defect states that were responsible for the broad emission spectra that were seen from 250–375 nm. Both the area under the curve and the full width at half maximum (FWHM) were found to increase as increasing concertation of Eu^{3+}. There is a small other peak (in the same broad region) formed due to doping. While increasing doping, the sharpness of the peak also increasing. The energy bandgap is decreasing while increasing concentration of Eu^{3+}. In order to determine the band gap $E_{g(host)}$ for $Ca_3LiZnV3O_{12}$, the formula is represented by equation (1). But, same formula cannot be applicable for Eu^{3+}-doped phosphor, because absorptions spectral of host and Eu^{3+} are overlap as shown in Figure. Hence to determine the band gap (E_g) accurately for $Ca_3LiZnV3O_{12}$:xEu^{3+} (x = 0.5, 1, 2, 3 and 5%), the formula is represented by equation (2) [23, 24].

$$E_{g(host)} = \frac{hc}{e\lambda} \ (eV) \quad \text{----------} \quad (1)$$

$$\alpha h\nu = B_d\left(h\nu - E_{g(Eu)}\right)^{n/2} \quad \text{----------} \quad (2)$$

Where α is absorption coefficient, B_d is a constant, $h\nu$ is the energy of incident photons, and n equals 1 to 4 for direct and indirect transitions, respectively. After taking log on both sides then we got a new formula which is represented by equation (3).

$$E_{g(Eu)} = \frac{hc}{e\lambda} - \left(\frac{\alpha hc}{e\lambda B_d}\right)^{2/n} \quad \text{----------} \quad (3)$$

For vanadate garnet phosphor, we got 3.72 eV (for 334 nm) while energy bandgap 3.5 eV, 3.42 eV, 3.37 eV, 3.25 eV and 3.11 eV for x = 0.5%, 1%, 2%, 3% and 5% respectively. Figure 8 shows the energy bandgap decreasing with increasing concertation.

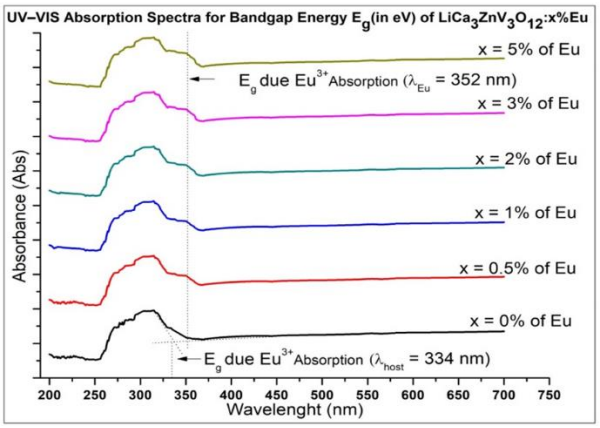

Figure 7: The UV–VIS absorbance spectra of $Ca_3LiZnV3O_{12}:xEu^{3+}$.

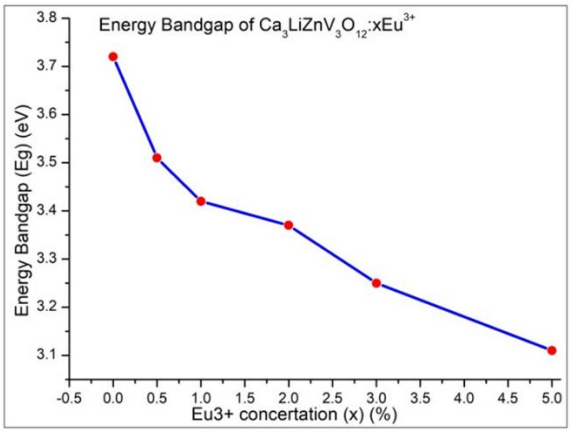

Figure 8: The variation energy bandgap with concertation of activators Eu3+ in $Ca_3LiZnV3O_{12}$.

3.6. Photoluminescence

In Figure 8(a), the excitation spectra of $LiCa_3ZnV_3O_{12}$ are monitored at 490 nm, and the phosphors of $LiCa_3ZnV_3O_{12}:Eu^{3+}$ are monitored at 611 nm. Both of these spectra are presented respectively. The excitation band was recorded from 200 to 400 nm. VO_4^{3-} groups have the excitation transition from $^1A1$ to $^1T_{1,2}$ [25]. Phosphors with the formula $LiCa_3ZnV_3O_{12}:Eu^{3+}$ has an excitation spectrum that is characterized by a broad excitation band. There is a clear Eu–O charge transfer band (CTB) at 292 nm in $LiCa_3ZnV_3O_{12}:Eu^{3+}$ samples, which demonstrates that electron transfer (ET) will take place from VO_4^{3-} groups to Eu^{3+} ions when the excitation wavelength is 344 nm [26].

Figure 8(b-e) illustrates the emission spectra of $LiCa_3ZnV_3O_{12}:Eu^{3+}$ phosphors those were stimulated by a wavelength of 344 nm wavelengths. Phosphors emit a broad emission from 400 nm to 570 nm due to VO_4^{3-} groups. It originates in emission from transitions of VO_4^{3-} groups from $^3T1_{,2}$ to $^1A_1$ [27]. In addition, samples that have been doped with Eu^{3+} exhibit a number of distinct peaks at wavelengths of 592 nm, 611 nm, and 633 nm. These peaks originate from the transitions of Eu3+ from $^5D_0$ to $^7F_{0,1,2,3}$ [28]. The energy transition diagram of $LiCa_3ZnV_3O_{12}:Eu^{3+}$ is shown in Figure 9(b). Figure 8(f) illustrates how the changes in emission intensities occur in response to changes in Eu^{3+} concentrations. At a concentration of 2%Eu^{3+}, the concentration quenching is achieved.

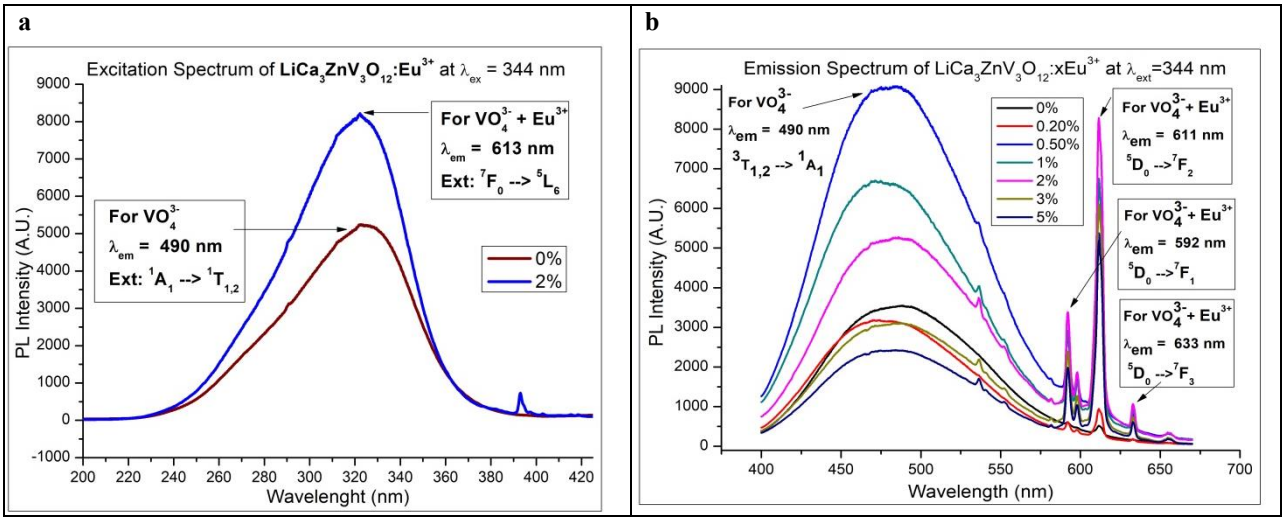

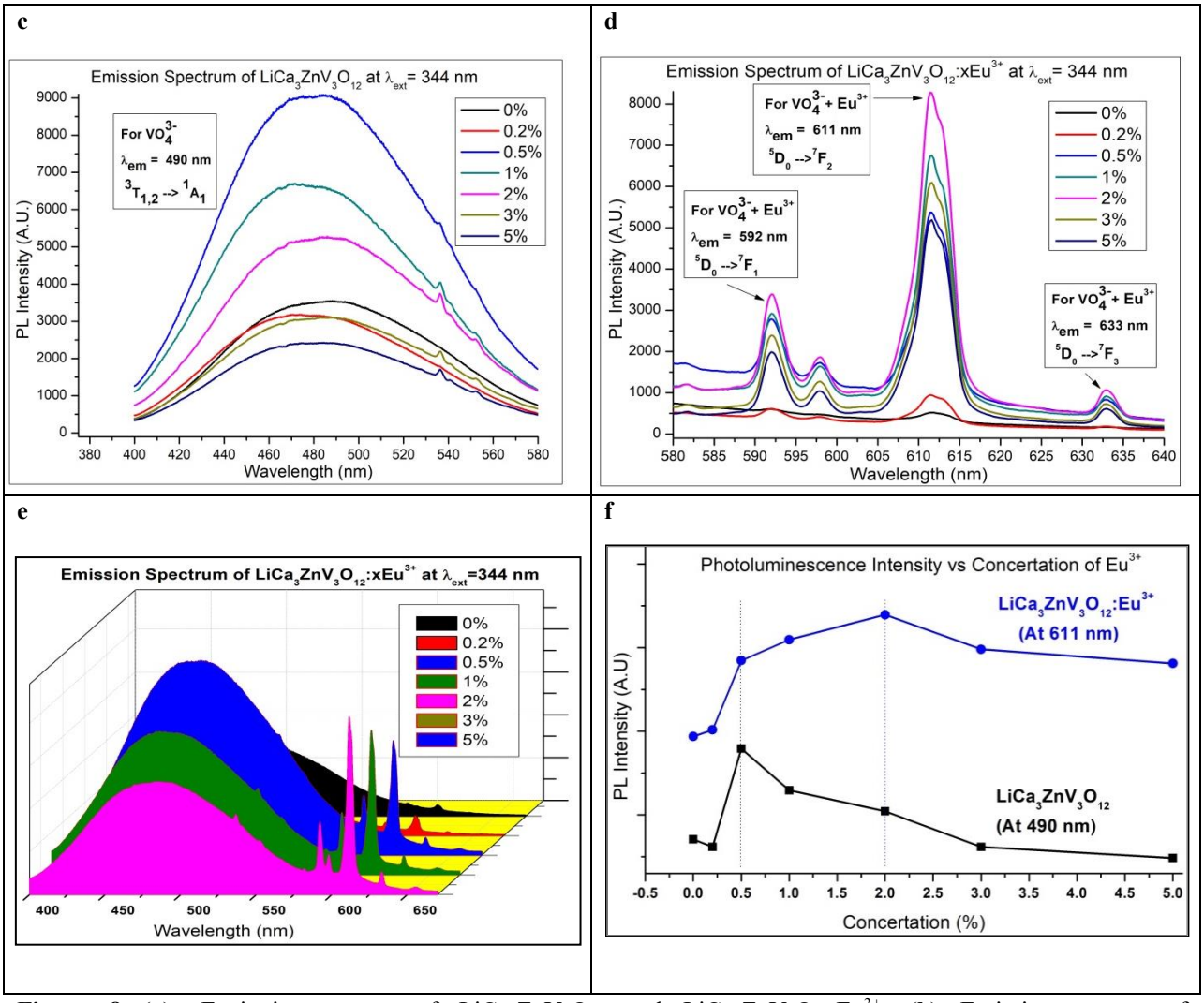

Figure 8 (a): Excitation spectra of $LiCa_3ZnV_3O_{12}$ and $LiCa_3ZnV_3O_{12}:Eu^{3+}$. **(b)** Emission spectra of $LiCa_3ZnV_3O_{12}:Eu^{3+}$. **(c)** Emission spectra due to VO_4^{3-}. **(d)** Emission spectra due to Eu^{3+}. **(e)** 3D view of emission spectra with concentrations of Eu^{3+}. **(f)** Variation of PL intensity due to concentrations of Eu^{3+}.

3.7. CIE Coordinators

As shown in Figure 9 (a), the CIE chromaticity diagram of $LiCa_3ZnV_3O_{12}:Eu^{3+}$ garnet-structured phosphor is visually represented. The sample has an emission spectrum that appears to be somewhere between blue and red regions. The chromaticity studies provide information about the color and the color coefficient that is dependent on temperature. The digital image of the CIE of the garnet structured phosphor that has been prepared draws its power from 6W and is illuminated by light with a wavelength of 356 nm. The color coordinates (x, y) of the $LiCa_3ZnV_3O_{12}$ are $(C_x, C_y) = (x, y) = (0.239, 0.329)$. This is true across the entire wavelength range, which extends from 400 nm to 700 nm. It has been observed that the color-dependent temperature for the obtained coordinates (CCT) is 17210 K. The arrow in the Figure 8(a), the changing in coordinates of $LiCa_3ZnV_3O_{12}:xEu^{3+}$ from x = 0.5 to 5%.

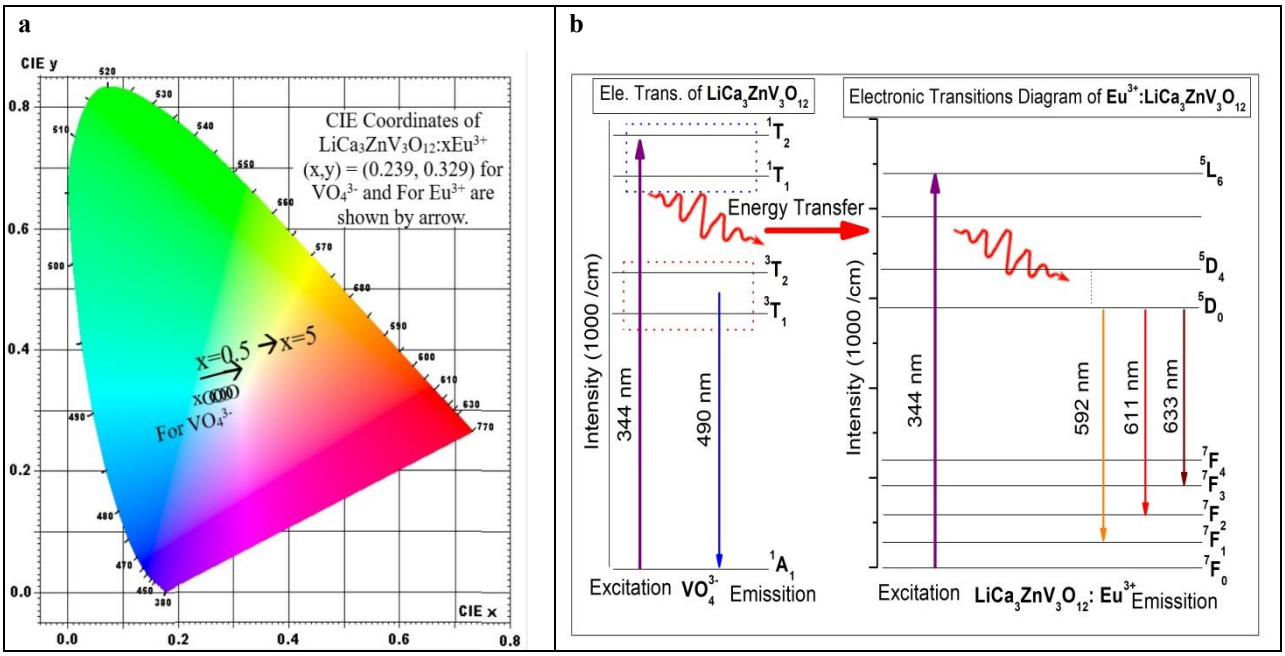

Figure 9 (a): Color coordinates calculation of $LiCa_3ZnV_3O_{12}:xEu^{3+}$. **(b)** Energy transitional diagram of $LiCa_3ZnV_3O_{12}:xEu^{3+}$.

4. Conclusion

$LiCa_3ZnV_3O_{12}:xEu^{3+}$ garnet phosphors were effectively synthesized by the SSR method which was sintering at 650 degrees Celsius for two hours and 950 degrees Celsius for six hours. The characterization techniques like XRD, SEM, EDX, FTIR, UV-VIS, and PL-spectra was used to study the phase, morphology, composition, bonds, energy bandgap and luminescence performance of vanadate garnet triggered by Eu3+ respectively. XRD study was investigated the single phase crystalline structure. This XRD was refined and we got low factors (R_p = 9.136, R_w = 7.364, R_{we} = 4.361, and χ^2 = 2.361). SEM images was displayed the morphological and topographical study. The composition of the prepared samples was confirmed by EDX. The energy bandgap of the prepared sample was calculated from UV-VIS spectra. As increasing concentration, there is decreeing energy bandgap. The thermal stability was studied by using TGA/DTA results. The nature of bonds among the metals with oxygen and bond length was studied by using FTIR spectra. The emission is obtained at 611 nm due to 2%Eu^{3+} and 490 due to VO_4^{3-} when this sample was excavated by UV- radiation of wavelength 344 nm. The CIE coordinates were also calculated by using digital photograph of the $LiCa_3ZnV_3O_{12}:Eu^{3+}$ which is found that (0.239, 0.329) for vanadate garnet. The applications of prepared phosphors in the production of red and blue lighting devices, white lighting devices, optical temperature sensors, active powder in solid-state lasers, and CRTs.

References:

[1] Berezovskaya, I. V., Z. A. Khapko, A. S. Voloshinovskii, N. P. Efryushina, S. S. Smola, and V. P. Dotsenko. "The effects of temperature and impurity phases on the luminescent properties of Ce3+-doped Ca3Sc2Si3O12 garnet." Journal of Luminescence 195 (2018): 24-30. https://doi.org/10.1016/j.jlumin.2017.11.002.

[2] Vandile , Ganesh, Deoram Nandanwar, and Amar Nandanwar. 2023. “A Review Synthesis and Luminescence Characterize of Emitting Phosphor of Garnet Structure With Effect of Heating Time”. Journal of Condensed Matter 1 (02):5-9. https://doi.org/10.61343/jcm.v1i02.19.

[3] Lohe, P. P., D. V. Nandanwar, P. D. Belsare, S. V. Moharil, S. P. Wankhede, and A. M. Badar. "Flux assisted synthesis of Ba9Sc2Si6O24: Eu2+ phosphor." In AIP Conference Proceedings, vol. 2352, no. 1. AIP Publishing, 2021. https://doi.org/10.1063/5.0053209.

[4] Vandile, G. C., Nandanwar D. V., Nandanwar A. K., Lohe P. P.. “The Optical and Structural Characteristics of the Series of Eu+3 – Doped Self-Activated Vanadate Garnet Phosphors”. ShodhKosh: Journal of Visual and Performing Arts (2024) 5 (7):739–747. https://doi.org/10.29121/shodhkosh.v5.i7.2024.4406.

[5] Vandile, G. C., Nandanwar D. V., Nandanwar A. K., Akhare D. W., “The Luminescence in Self Activated and Sm3+ Rich Garnet Phosphor Sr2NaZn2V3O12 Prepared by Solid-State Reaction”, J. Cond. Matt. 2024; 02 (02): 104-109, https://doi.org/10.61343/jcm.v2i02.87.

[6] Nandanwar, A. K., Sarkar N. N., Sahu D. K., Choudhary D. S., Rewatkar K. G., "Effect of Ni+ 2 substitution on structural and electrical behaviour of nano-size cadmium ferrites." Materials Today: Proceedings 5, no. 10 (2018): 22669-22674. https://doi.org/10.1016/j.matpr.2018.06.643.

[7] Bharat, L. Krishna, Soo-Kun Jeon, Kurugundla Gopi Krishna, and Jae Su Yu. "Rare-earth free self-luminescent Ca2KZn2 (VO4) 3 phosphors for intense white light-emitting diodes." Scientific Reports 7, no. 1 (2017): 42348. https://doi.org/10.1038/srep42348.

[8] G. Gundiah, Y. Shimomura, N. Kijima, A.K. Cheetham, Novel red phosphors based on vanadate garnets for solid state lighting applications, Chem. Phys. Lett. 455 (2008) 279–283, https://doi.org/10.1016/j.cplett.2008.02.083.

[9] T. Hasegawa, Y. Abe, A. Koizumi, T. Ueda, K. Toda, M. Sato, Bluish-White Luminescence in Rare-Earth-Free Vanadate Garnet Phosphors: Structural Characterization of LiCa3MV3O12 (M =Zn and Mg, Inorg. Chem. 57 (2018) 857–866, https://doi.org/10.1021/acs.inorgchem.7b02820.

[10] G. Blasse, Energy transfer in oxidic phosphors, Phys. Lett. A 28 (1968) 444–445, https://doi.org/10.1016/0375-9601(68)90486-6.

[11] R. Cao, T. Chen, Y. Ren, C. Liao, Z. Luo, Y. Ye, Y. Guo, Tunable emission of LiCa3MgV3O12: Bi3+via energy transfer and changing excitation wavelength, Mater. Res. Bull. 111 (2019) 87–92, https://doi.org/10.1016/j.materresbull.2018.11.011.

[12] Gopal Warutkar, Nilesh Ugemuge, Shruti Dhale, Priya V. Tumram, P.K. Tawalare, Renuka Nafdey, S.V. Moharil, Host sensitized mid-infrared emission in LiCa3MgV3O12 activated with Er3+, Emergent Mater. (2024) 1–7, https://doi.org/10.1007/s42247-024-00819-6.

[13] Warutkar, Gopal N., N. S. Ugemuge, Ashvini Pusdekar, Shruti Dhale, Khushbu Sharma, Babasaheb R. Sankapal, Shilpa Kulkarni, and S. V. Moharil. "Near IR emission in garnet structured LiCa3MgV3O12: Nd3+ phosphor." Optik 322 (2023): 172180. https://doi.org/10.1016/j.ijleo.2024.172450.

[14] P. Dang, S. Liang, G. Li, Y. Wei, Z. Cheng, H. Lian, J. Lin, Full color luminescence tuning in Bi3+/Eu3+-doped LiCa3MgV3O12 garnet phosphors based on local lattice

distortion and multiple energy transfers, Inorg. Chem. 57 (2018) 9251–9259, https://doi.org/10.1021/acs.inorgchem.8b01271.

[15] Lohe, P. P., D. V. Nandanwar, P. D. Belsare, and S. V. Moharil. "Recent developments in white light emitting diodes." In AIP Conference Proceedings, vol. 1953, no. 1. AIP Publishing, (2018). https://doi.org/10.1063/1.5032834.

[16] Mihóková, E., V. Babin, V. Jarý, L. Havlák, M. Buryi, and M. Nikl. "Defect states and temperature stability of Eu2+ center in Eu-doped yttrium aluminum garnet." Journal of Luminescence 190 (2017): 309-313. https://doi.org/10.1016/j.jlumin.2017.05.065.

[17] Qin, Xian, Xiaowang Liu, Wei Huang, Marco Bettinelli, and Xiaogang Liu. "Lanthanide-activated phosphors based on 4f-5d optical transitions: theoretical and experimental aspects." Chemical reviews 117, no. 5 (2017): 4488-4527. https://doi.org/10.1021/acs.chemrev.6b00691.

[18] Kim, Sun Woog, Kenji Toda, Takuya Hasegawa, Kazuyoshi Uematsu, and Mineo Sato. "Color Tuning of Oxide Phosphors." Phosphors, Up Conversion Nano Particles, Quantum Dots and Their Applications: Volume 1 (2017): 219-246. https://link.springer.com/chapter/10.1007/978-3-662-52771-9_7.

[19] Jia, Dongdong, and Xiao-jun Wang. "Alkali earth sulfide phosphors doped with Eu2+ and Ce3+ for LEDs." Optical Materials 30, no. 3 (2007): 375-379. https://doi.org/10.1016/j.optmat.2006.11.061.

[20] Li, Guogang, Ying Tian, Yun Zhao, and Jun Lin. "Recent progress in luminescence tuning of Ce^{3+} and Eu^{2+}-activated phosphors for pc-WLEDs." (2015). DOI:https://doi.org/10.1039/C4CS00446A.

[21] Li, Jinkai, Ji-Guang Li, Zhongjie Zhang, Xiaoli Wu, Shaohong Liu, Xiaodong Li, Xudong Sun, and Yoshio Sakka. "Gadolinium Aluminate Garnet (Gd3Al5O12): Crystal Structure Stabilization via Lutetium Doping and Properties of the (Gd 1− x Lu x) 3 Al5O12 Solid Solutions (x= 0–0.5)." Journal of the American Ceramic Society 95, no. 3 (2012): 931-936. https://doi.org/10.1111/j.1551-2916.2011.04991.x.

[22] Lanez, I., B. Rekik, M. Derbal, and A. Chaib. "Structural study and the effect of ionic size of the systems (Gd1-x Lux) 3Al5 O12 doped erbium." Journal of Fundamental and Applied Sciences 11, no. 2 (2019): 857-874. https://www.ajol.info/index.php/jfas/article/view/247103.

[23] Li, Ji-Guang, Xiaodong Li, Xudong Sun, Takayasu Ikegami, and Takamasa Ishigaki. "Uniform colloidal spheres for (Y1− x Gd x) 2O3 (x= 0–1): Formation mechanism, compositional impacts, and physicochemical properties of the oxides." Chemistry of Materials 20, no. 6 (2008): 2274-2281. https://doi.org/10.1021/cm7033257.

[24] Zhang, Liangliang, Dandan Wang, Zhendong Hao, Xia Zhang, Guo-hui Pan, Huajun Wu, and Jiahua Zhang. "Cr3+-doped broadband NIR garnet phosphor with enhanced luminescence and its application in NIR spectroscopy." Advanced Optical Materials 7, no. 12 (2019): 1900185. https://doi.org/10.1002/adom.201900185.

[25] Zhou, Jiangcong, Feng Huang, Ju Xu, Hui Chen, and Yuansheng Wang. "Luminescence study of a self-activated and rare earth activated Sr 3 La (VO 4) 3 phosphor potentially applicable in W-LEDs." Journal of Materials Chemistry C 3, no. 13 (2015): 3023-3028. DOI: 10.1039/D3DT03138A.

[26] Hakeem, D. A., J. W. Pi, S. W. Kim, and K. Park. "New Y 2 LuCaAl 2 SiO 12: Ln (Ln= Ce 3+, Eu 3+, and Tb 3+) phosphors for white LED applications." Inorganic Chemistry Frontiers 5, no. 6 (2018): 1336-1345. DOI: 10.1039/D3TC00921A.

[27] Zhou, Jiangcong, Feng Huang, Ju Xu, Hui Chen, and Yuansheng Wang. "Luminescence study of a self-activated and rare earth activated Sr 3 La (VO 4) 3 phosphor potentially applicable in W-LEDs." Journal of Materials Chemistry C 3, no. 13 (2015): 3023-3028. DOI: 10.1039/D3DT03138A.

[28] Hu, Taotao, Wenzhi Huang, Ruiqi Zhong, Jindong Zhang, Na Zeng, Yangyang Wang, and Wanyu Liu. "Crystal growth behavior and fluorescence properties of LaMgAl11O19: Eu3+ nano-powders prepared via sol-gel process." Ceramics International 49, no. 7 (2023): 10554-10565. https://doi.org/10.1016/j.ceramint.2022.11.242.